Array Antenna Characterization Technique Based on Evanescent Reactive-Near-Field Probing in an Ultra-Small Anechoic Box

Qing Han, Keizo Inagaki, and Takashi Ohira

ATR Adaptive Communications Research Laboratories, 2-2-2 Hikaridai, Keihanna Science City, Kyoto 619-0288, Japan

Abstract — **This paper presents a new technique in which small array antenna performance is characterized based on reactive-near-field probing in an ultra-small anechoic box and with a multi-probe. Unlike conventional far- or near-field measurement methods, the radiation patterns in the proposed approach are computed from the currents only at discrete points picked up in the evanescent region of an array antenna's elements. An equivalent weight vector is introduced to effectively eliminate the need for sensor scanning. Cross correlation coefficients between the far-field patterns of a conventional measurement and the reactive-near-field ones are as high as 0.933 to 0.998 for single-probe pick-up and as high as 0.885 to 0.988 for multi-probe pick-up. This shows that the proposed technique can replace large anechoic chambers currently used for characterizing small array antennas' performance.**

I. Introduction

In the design of any antenna, it is of the utmost importance to accurately measure its performance in order to verify its suitability for the intended application. Antenna measurements, such as radiation pattern, gain, and radiation efficiency, are usually conducted in a large anechoic chamber, in order to avoid reflections from nearby objects that would affect the field pattern. The construction and maintenance of large anechoic chambers is very expensive and requires considerable space. It would be particularly unreasonable to have to invest in a large chamber to measure a small, low-cost antenna. Therefore, it is desirable to decrease the chamber's size. However, there are two limiting factors that determine the size of a chamber. One is the size of the absorbers and the clearance needed between the antenna and the absorber, and the other is the minimum possible distance between the antenna under test (AUT) and the measurement antenna.

To overcome the first limitation, we have investigated the influence of RF absorbers in the vicinity of an antenna and found the minimum distance between the antenna and the absorber [1]. To overcome the second limitation, a number of researchers have made efforts to investigate the minimum distance between the two antennas [2]-[3]. Unfortunately, since they employed two antennas in the chamber to perform conventional measurements, the size reduction of the chamber was limited to the antenna separation distance.

In attempts to conduct reactive-near-field measurements, an example of aperture array antenna was reported in [4] and an optically modulated scatter used as an electric-field probe was developed in [5]. However, the reflections from nearby objects and the positioners are still unsolved problems.

This paper proposes a new technique for array antenna characterization. This involves reactive-near-field measurement in the evanescent region using low-interference microwave current probes. We introduce an Equivalent Weight Vector (EWV) that effectively eliminates the need for sensor scanning. This feature gives our evanescent-region approach a quite superior advantage over conventional near-field techniques that are generally carried out in the Fresnel region instead. Applying this advantage, we successfully characterize a 2.4-GHz rod array antenna radiation pattern in an ultra-small anechoic box.

II. Principle Of Measurement

A. Equivalent Weight Vector

Generally speaking, the far-field directivity pattern of a current-based antenna is calculated as

$$D_f(\theta,\phi)=\frac{j\omega\mu}{4\pi}\int_v J\frac{1}{r}e^{j\beta r}dv \qquad (1)$$

where J is the density of current on the antenna, r is the distance from the antenna, β is the propagation constant, and v is the volume of integration. It is common to do a volume or closed surface integration according to (1) to deduce a far-field pattern from a near-field measurement. Needless to say, a great many points have to be measured. As a result, the measurement and computation time may make near-field measuring unattractive for antennas that are relatively large electrically. Therefore, we propose a method in which the current is measured only at discrete points. Since the element factor is approximately the same

0-7803-7695-1/03/$17.00 © 2003 IEEE

as a single rod, the directivity is dominated by its array factor

$$D_a(\theta,\phi) = \boldsymbol{i}^T \boldsymbol{a} \quad (2)$$

where, $\boldsymbol{i} = [i_0, i_1, \cdots, i_n]^T$, $a = [a_0, a_1, \cdots, a_n]^T$,

$\boldsymbol{a}_k = \exp\{j\beta \boldsymbol{r}_k^T [\cos\theta\cos\phi, \cos\theta\sin\phi, \sin\theta]^T\}$,

$\boldsymbol{i}$ equivalently plays the role of weight vector [6], $\boldsymbol{a}$, $\boldsymbol{r}_k$ (k=0 to n), θ, and ϕ are array's steering vector, position vector, elevation angle, and azimuth angle, respectively. It is clear that the antenna's directivity can be easily understood as long as the EWV or element currents are given since the other parameters in (2) are known variables.

B. Reactive Near Field

Electromagnetic fields associated with an antenna are divided into three regions: far-field, near-field, and reactive-near-field [7]. We only give a brief explanation of the reactive-near-field region here. The region nearest to the antenna is the reactive-near-field or evanescent region. Its electromagnetic energy decays very rapidly with distance ($1/r^3$). The reactive-near-field region includes both nonpropagating (reactive) and propagating energy.

Near-field measurements are generally made outside of the evanescent region. Otherwise, higher sampling densities and separate E and H field measurements would be required. On the one hand, because the electromagnetic coupling between the individual elements of an array antenna is strong and the contribution from each element is integrated and difficult to separate, we would prefer to take measurements in close proximity to each element. However, on the other hand, conducting a reactive-near-field measurement would likely make it impossible for us to ignore the influence that the probe has on the antenna characteristics. Fortunately, extensive research has been done on low-interference probes, such as the multilayered magnetic field probe [8], the Electro-Optic (EO) probe [9], and the Magneto-Optic (MO) probe [10]. These probes not only exhibit little interference on electromagnetic fields, but also have a high E and H field separation property and therefore are an adequate solution to the problem.

C. Single-Probe Pick-Up

A single-probe pick-up is used to detect the elements one by one. Although the single-probe is simple, it is time-consuming to use and requires troublesome positioning especially in the case where a large number of antennas need to be measured.

D. Multi-Probe Pick Up

To shorten the experiment time and avoid the troublesome positioning, we designed a multi-probe to pick up the reactive-near-field of all antenna elements simultaneously. Figure 1 shows an example of a 7-element array antenna consisting of a center element and 6 surrounding elements. The symbols e#n, p#n and c#n (n = 0 to 6) in Fig. 1 represent elements, probes, and cables, respectively. In this configuration, we found that p#0 influenced the results of its two neighboring probes. In addition to the former influence, there were also errors caused by using different probes and different cables in the multi-probe measurement. We do not intend to discuss the influence of the probe in this paper, but we will calibrate the errors caused by different probes and cables. As a result, the measurements using the multi-probe were made in two steps. First, we measured the center element (e#0) with p#0 while the other probes point to their corresponding elements. Second, we simultaneously measured the surrounding elements with p#1 to p#6 and adjust the p#0 offset from the array antenna, as shown in Fig. 2.

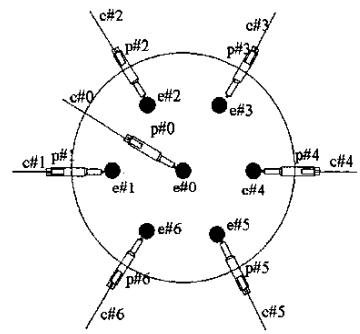

Fig. 1. Simultaneous multi-probe measurement of the 7-element currents.

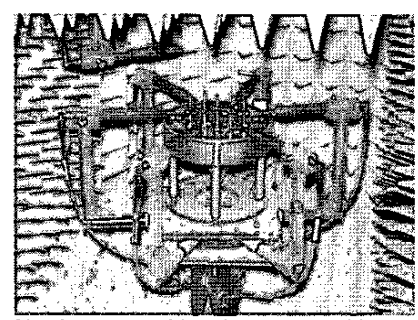

Fig. 2. Simultaneous multi-probe constructed in an ultra-small anechoic box.

The interior receivers of a network analyzer (e.g., A, B, R1, and R2 in Agilent E8358A) were used to evaluate the measurement results. When p#0 and c#0 were chosen as the standard probe and cable we obtained the calibration

data according to the simple flow chart below. Once the calibration data are obtained, they can be applied to continuous measurements until the probes and cables are changed.

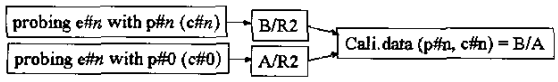

III. Measuring System

In order to measure the antenna element currents, we configured a measuring system, as shown in Fig. 3, which consisted of an ultra-small anechoic box, probes, positioners, and a 6-way switch, in addition to auxiliary equipment.

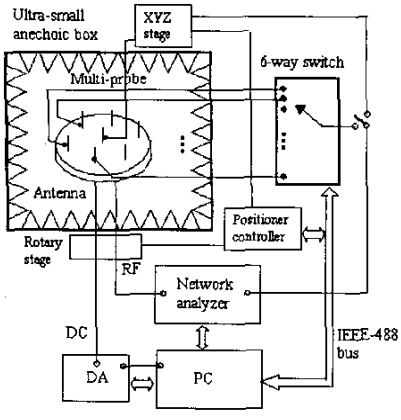

Fig. 3. An ultra-small anechoic measuring system for probing reactive-near-fields of array antennas.

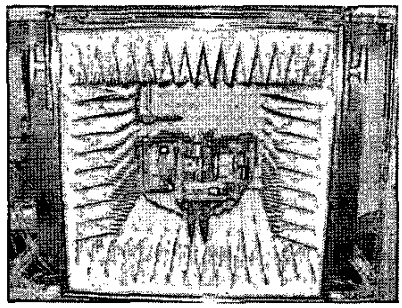

Fig. 4. A prototype ultra-small anechoic box with an array antenna and current-probes

Figure 4 shows a fabricated, cubic, ultra-small anechoic box with the front door opened. Its size is 63 cm × 63 cm × 63 cm. The 11.4 cm-thick pyramid absorbers are attached to six faces inside the box. Only the probes and the AUT are placed in the box. Other instruments, even including the positioners, are placed outside the box to reduce the reflections.

A multilayered magnetic field probe was chosen for this work because it is cheaper, simpler and easier to use than the other low-interference probes. Positioners consisting of motor and manual stages provide six-axes movement to meet the requirements of a cylindrical array antenna. The system uses a PC interfaced with a positioner controller, network analyzer, switch controller, and digital to analog (DA) converter via an IEEE-488/GP-IB bus to achieve a fully automated magnitude and phase measurement.

IV. Results

The AUT is a 7-element ESPAR (Electronically Steerable Parasitic Array Radiator) antenna [6]. One fed element is surrounded by six parasitic elements loaded with varactors at their base. The variable reactance controlled by bias voltages alters the performance of the antenna so directional beams can be steered through a 360° azimuth. In the measurement, the relatively strong magnetic field at the bottom of each ESPAR antenna element was measured and the distance between the element and probe was 0. Figures 5 (a) to (c) (see below) show the radiation patterns that were obtained by applying the currents measured here to (2). However, the position vector in (2) becomes $r_k=[d\cos((k-1)\pi/3, -d\sin((k-1)\pi/3), 0)^T$, while d is the distance between the antenna elements. Figure 5 (a) shows the omni pattern obtained by restricting the bias voltages of the six parasitic elements of the ESPAR antenna to 20 volts, while (b) and (c) show two beam patterns separated by 240°. The solid, dashed, and dotted lines represent the results of a multi-probe pick-up, a single-probe pick-up, and a conventional far-field measurement, respectively. Both the omni and beam patterns show good agreement. To evaluate these agreements in quantity, we defined a cross correlation coefficient as

$$\rho = \frac{\oint D_a(\theta,\phi) D_f(\theta,\phi)^* \, d\theta d\phi}{\sqrt{\oint |D_a(\theta,\phi)|^2 \, d\theta d\phi} \sqrt{\oint |D_f(\theta,\phi)|^2 \, d\theta d\phi}},$$

where $D_a(\theta, \phi)$ represents the array factor as described in (2) and $D_f(\theta, \phi)$ is the far-field pattern obtained by direct measurement in a large chamber. The superscript * denotes a complex conjugate. The value of ρ falls in $0 \le |\rho| \le 1$. The cross correlation coefficients of several omni and beam patterns were calculated and are shown in Table I. Omni patterns exhibited cross correlation coefficients higher than 0.998 and beam patterns higher than 0.933 for the single-probe pick-up. For multi-probe pick-up, the cross correlation coefficients of the omni patterns were 0.986 to 0.988 and those of the beam patterns were 0.885 to 0.936.

TABLE I CROSS CORRELATION COEFFICIENTS

Beam direction	$\|\rho\|$ (Single-probe)	$\|\rho\|$ (Multi-probe)
Omni (0V)	0.994	0.994
Omni (20V)	0.998	0.997
0°	0.933	0.839
60°	0.952	0.834
120°	0.956	0.891
180°	0.945	0.881
240°	0.958	0.876
300°	0.946	0.840

V. CONCLUSION

A new technique for array antenna characterization was proposed. Reactive-near-field measurement in the evanescent region using low-interference multi-probes and an equivalent weight vector that effectively eliminates the need for sensor scanning were introduced. The technique, with its quite superior advantage over the conventional near-field techniques that are generally carried out in the Fresnel region, was applied successfully to characterize a 2.4-GHz rod array antenna in an ultra-small anechoic box. Far-field radiation patterns obtained by the approach proposed in this paper were compared with those obtained directly from far-field measurement. They showed good agreement. Furthermore, cross correlation coefficients calculated between reactive-near-fields results and direct far-field measurement results were as high as 0.933 to 0.998 for a single-probe pick-up and as high as 0.885 to 0.988 for a multi-probe pick-up. We conclude that the proposed technique will replace conventional methods for characterizing small array antennas' performance.

ACKNOWLEDGEMENT

The authors wish to express their sincere gratitude to Dr. B. Komiyama for his enthusiastic encouragement of this study. This research was supported in part by the Telecommunications Advancement Organization of Japan.

REFERENCES

[1] Q. Han, K. Inagaki, K. Iigusa, R. Schlub, and T. Ohira, "Reactive-field anechoic box for ESPAR antenna measurement," *IEICE Trans. Electron.*, E85-C, 7, pp. 1451-1459, July 2002.

[2] D. Geen and D. Smith, "Design, construction and performance of a small, low cost anechoic measuring system for research applications," *IEEE AP-S International Symposium*, pp. 1738-1741, 1995.

[3] C. Icheln, J. Ollikainen, and P. Vainikainen, "Effects of RF absorbers on measurements of small antennas in small anechoic chambers" *IEEE AESS Systems Magazine*, pp. 17-20, Nov. 2001.

[4] J. Sato, U. Sangawa, and N. Adachi, "Analysis method for aperture field distribution of array antennas using near-field measurement," *IEICE General Conference Proc.*, B-1-226, p. 242, March. 2002.

[5] W. Liang, G. Hygate, J. F. Nye, D. G. Gentle, and R. J. Cook, "A probe for making near-field measurements with minimal disturbance: the optically modulated scatter," *IEEE Trans. On Antenna and Propagation*, Vol. 45, No. 5, pp. 772-780, May 1997.

[6] T. Ohira and K. Gyoda, "Hand-held microwave direction-of arrival finder based on varactor-tuned analog aerial beamforming," *Proc. of APMC2001*, Vol. 2 of 3, pp. 585-588, Dec. 2001.

[7] A. D. Yaghjian, "An overview of near-ficld antenna measurement," *IEEE Trans. On Antenna and Propagation*, Vol. AP-34, No. 1, pp. 30-45, Jan. 1986.

[8] N. Masuda, N. Tamaki, T. Watanabe, and K. Ishizaki, "A miniature high-performance magnetic-field probe for measuring high-frequency currents," *NEC Res.*, Vol. 42, No. 2, pp. 246-250, April 2001.

[9] T. Nagatsuma, "Electro-optic testing technology for high-speed LSIs," *IEICE Trans. Elec.*, Vol. E79-C, No. 4, pp. 482-488, April 1996.

[10] S. Wakana, T. Ohara, M. Abe, E. Yamazaki, M. Kishi, and M. Tsuchiya, "Fiber-edge electrooptic/magnetooptic probe for spectral-domain analysis of electromagnetic field," *IEEE Trans. on MTTs*, Vol. 48, No. 12, pp. 482-488, Dec. 1996.

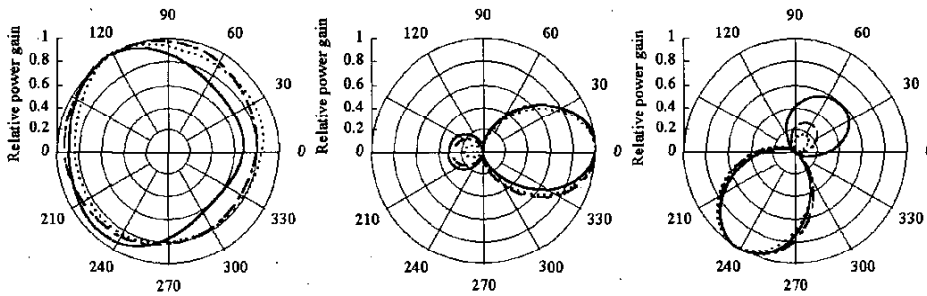

Fig. 5. Linear-scale power patterns for three different ESPAR antennas